# Radiation Absorbed Dose Estimates for [1-Carbon-11]-Glucose in Adults: The Effects of Hyperinsulinemia

William J. Powers

*Departments of Neurology and Radiology, Washington University School of Medicine and the Lillian Strauss Institute for Neuroscience of the Jewish Hospital of St. Louis, St. Louis, Missouri*

As preparation for studies of blood-brain glucose transport in diabetes mellitus, radiation absorbed dose estimates from intravenous administration of [1-$^{11}$C]-glucose for 24 internal organs, lens, blood and total body were calculated for three physiologic conditions: euinsulinemic euglycemia, hyperinsulinemic euglycemia and hyperinsulinemic hyperglycemia. **Methods:** Cumulated activities in blood, insulin-independent and insulin-dependent compartments were calculated from blood time-activity curves in normal human volunteers and macaques. Apportionment of cumulated activity to individual organs in insulin-dependent and insulin-independent compartments was based on previously published data. Absorbed doses were calculated with the computer program MIRDOSE 3 for the 70-kg adult phantom. S for blood was calculated separately. **Results:** The heart wall, lungs and spleen were the organs receiving the highest dose. The effect of hyperinsulinemia was demonstrated by the increase in absorbed dose to the muscle, heart and blood with a decrease to other internal organs. This effect was more pronounced during hyperinsulinemic hyperglycemia. Hyperinsulinemia produced a decrease in effective dose due to the decrease in cumulated activity in organs with specified weighting factors greater than 0.05. **Conclusion:** The effective dose per study for [1-$^{11}$C]-glucose is comparable to that reported for 2-deoxy-[2-$^{18}$F]-glucose.

**Key Words:** [1-$^{11}$C]-glucose; PET; absorbed dose

**J Nucl Med 1996; 37:1668–1672**

Measurement of regional brain glucose metabolism (CMRGlc) with PET using 2-deoxy-[2-$^{18}$F]-glucose ($^{18}$FDG) or 2-deoxy-[1-$^{11}$C]-glucose ($^{11}$CDG) has been valuable for providing insight into the metabolism of normal and diseased human brains (*1–4*). Both deoxyglucose and fluorodeoxyglucose are glucose analogs. Accurate determination of CMRGlc requires a priori knowledge of the ratio between analog uptake and glucose uptake (the lumped constant). The value of this constant changes under different physiological and pathological conditions such as ischemia, hypoglycemia and immaturity (*5–10*).

This problem with glucose analogs can be avoided by the use of glucose itself as the radiotracer. Measurements of CMRGlc with photosynthetically prepared [$^{11}$C]-glucose have been hampered by methods that do not adequately account for the early efflux from the brain of [$^{11}$C]-$CO_2$ and other [$^{11}$C]-metabolites (*11–14*). Use of [$^{11}$C]-glucose labeled specifically at the 1-carbon position ([1-$^{11}$C]-glucose) has the advantage that loss of [$^{11}$C]-$CO_2$ is only 0.5% per minute (*15*). We and others have begun to use this tracer to study various aspects of cerebral physiology with PET (*16–18*). Among the most interesting and controversial of these aspects is the effect of diabetes mellitus on blood-to-brain glucose transport and CMRGlc. To study this issue properly requires consideration of the effects of insulin and hyperglycemia as well as the disease itself. Safe performance of such research in human subjects necessitates accurate knowledge of the radiation absorbed dose after intravenous administration of [1-$^{11}$C]-glucose (1-$^{11}$CG) and the changes in absorbed dose caused by hyperinsulinemia and hyperglycemia.

Received Aug. 16, 1995; revision accepted Dec. 13, 1995.

For correspondence or reprints contact: William J. Powers, MD, East Building Imaging Center, Washington University School of Medicine, 4525 Scott Ave., Campus Box 8225, St. Louis, MO 63110.

## MATERIALS AND METHODS

Mean absorbed dose for individual organs was calculated according to the MIRD scheme (*19*):

$$\bar{D}(r_k) = \sum_{h=1}^{n} \tilde{A}_h S(r_k \leftarrow r_h)$$

$$S(r_k \leftarrow r_h) = \Delta_p \Phi_p(r_k \leftarrow r_h) + \Delta_{np} \Phi_{np}(r_k \leftarrow r_h)$$

$\bar{D}(r_k)$ is the mean absorbed dose to target organ $r_k$ (Gy), $\tilde{A}_h$ is the cumulated activity in source organ $r_h$ (Bq sec), $S(r_k \leftarrow r_h)$ is the mean absorbed dose per unit cumulated activity (Gy Bq$^{-1}$ sec$^{-1}$) from the source organ $r_h$ irradiating target organ $r_k$, $\Delta_p$ is mean energy emitted per unit cumulated activity (kg Gy Bq$^{-1}$ sec$^{-1}$) for penetrating radiation (511 keV annihilation photons), $\Phi_p(r_k \leftarrow r_h)$ is specific absorbed fraction (kg$^{-1}$) for penetrating radiation from source organ $r_h$ irradiating target organ $r_k$, $\Delta_{np}$ is the mean energy emitted per unit cumulated activity (kg Gy Bq$^{-1}$ sec$^{-1}$) for nonpenetrating radiation (positrons), $\Phi_{np}$ ($r_k \leftarrow r_h$) is specific absorbed fraction (kg$^{-1}$) for nonpenetrating radiation from source organ $r_h$ irradiating target organ $r_k$.

### Calculation of Cumulated Activities

The half-life of $^{11}$C was obtained from Weber et al. (*20*).

*Urinary Loss.* In normal adults, no glucose appears in the urine until plasma concentrations exceed 10 m*M* due to complete tubular reabsorption of the glucose filtered by the glomeruli (*21*). Segal et al. (*22*) recovered only 1%–2% of administered activity in the urine within a 24-hr period after intravenous administration of [1-$^{14}$C]-glucose in normal adults. In subjects with diabetes mellitus, the plasma glucose threshold for urinary excretion is, if anything, higher due to the presence of glomerular disease that reduces the filtered load (*21*).

*Pulmonary [$^{11}$C]-$CO_2$.* Segal et al. (*22*) measured the loss of [$^{14}$C]-$CO_2$ from the lungs of normal adult volunteers after intravenous administration of [1-$^{14}$C]-glucose as 9% of the administered activity ($A_o$) per hour. This can be equated to the rate constant for pulmonary washout of a gas to determine $\tilde{A}$ for pulmonary [$^{11}$C]-$CO_2$ (*23,24*) (Table 1).

*Clearance from Blood to Tissues.* Ferrannini and colleagues (*25*) modeled the clearance of glucose from blood to tissue based on studies of [3-$^{3}$H]-D-glucose. They identified a rapidly equilibrating, insulin-independent compartment (brain, splanchnic organs, kidneys) that accounted for 0.68–0.77 of glucose consumption and a slowly equilibrating, glucose-dependent compartment (muscle

**TABLE 1**
Total Cumulated Activity*
(MBq-hr per MBq $A_0$)

| | EI/EG | HI/EG | HI/HG |
|---|---|---|---|
| Lungs ($[^{11}C]$-$CO_2$) | 0.0005 | 0.0005 | 0.0005 |
| Blood | 0.1241 | 0.1854 | 0.2272 |
| Heart and muscle | 0.0512 | 0.1740 | 0.2203 |
| Internal organs | 0.2942 | 0.1101 | 0.0220 |

*Does not include respiratory loss of $[^{11}C]$-$CO_2$.
EI/EG = euinsulinemic euglycemia; HI/EG = hyperinsulinemic euglycemia; HI/HG = hyperinsulinemic hyperglycemia.

and heart) that accounted for the remaining 0.23–0.32. Ikkos and Luft (*26*) analyzed glucose disappearance from blood after an intravenous load. They report a double exponential curve with a rapid component requiring 25–30 min for equilibration and a slow component with a time constant of 0.013–0.014 $min^{-1}$ in normals and 0.003–0.007 $min^{-1}$ in diabetics.

I analyzed blood time-activity curves collected for 22.8–24.6 min after intravenous bolus administration of photosynthetically prepared $[^{11}C]$-glucose in six normal volunteers, aged 18–46. Decay-corrected curves could be resolved into double exponentials with fast and slow components (Fig. 1). The slow component was fit first from 10 min to the end of the curve. It had a half-time of 40.05 ± 14.15 min for an mean time constant of 0.017 $min^{-1}$ (1.04 $hr^{-1}$), similar to that of 0.013–0.014 $min^{-1}$ reported by Ikkos and Luft (*26*). The fraction of administered activity in the slow compartment was calculated by extrapolating the fitted curve to the time of peak of the time-activity curve and recording the blood activity at this time. Assuming a blood volume of 5 liters (*27*), the fraction of the administered activity was determined as 0.332 ± 0.061. This agrees well with values of 0.23–0.32 for the fraction of glucose uptake that goes to heart and muscle reported by Ferrannini et al. (*25*). The half-time of the residual portion of the curve was then determined by fitting from the peak time as 1.29 ± 0.501 min for a mean time constant of 0.537 $min^{-1}$ (32.24 $hr^{-1}$).

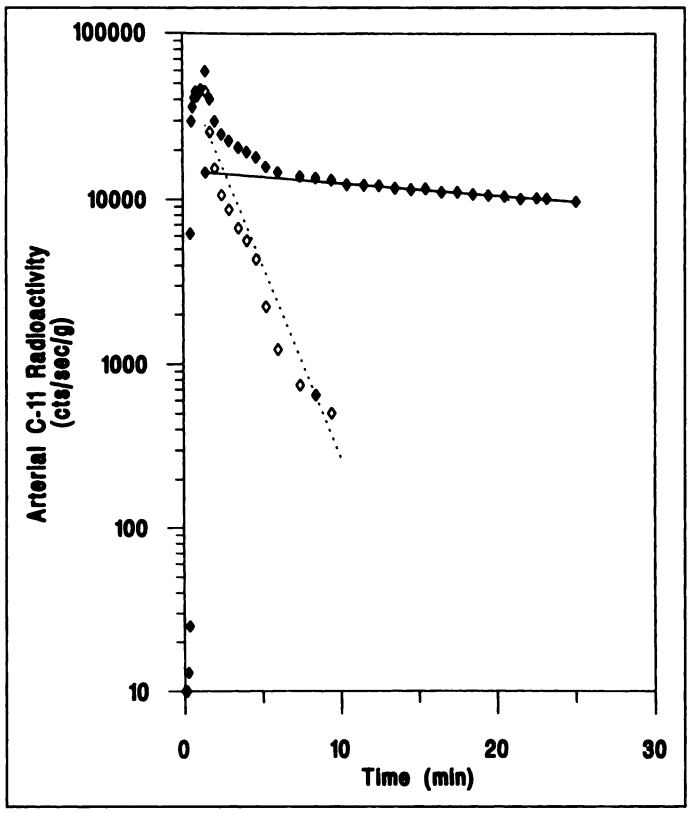


**FIGURE 1.** Semilogarithmic plot of decay-corrected arterial blood time-activity curve (♦) from a 22-yr-old normal male volunteer after injection of 592 Mbq (16 mCi) of photosynthetically prepared $^{11}$C-D-glucose. The curve is resolved by stripping into a slow component with a T½ of 41.3 min (solid line) and a fast component (◇) with T½ of 1.28 min (dotted line).

Based on these data, the clearance of 1-$^{11}$CG from blood to extravascular tissue in euinsulinemic, euglycemic normal adults can be described by a slow, insulin-dependent component to heart and muscle comprising $0.332A_0$ with a rate constant of 1.04 $hr^{-1}$ and a fast, insulin-independent component to other organs comprising the remaining $0.668A_0$ with a rate constant of 32.24 $hr^{-1}$.

During hyperinsulinemic euglycemia, muscle glucose uptake increases to 0.70–0.75 of total-body glucose uptake (*28,29*). During hyperinsulinemic hyperglycemia, this fraction increases to 0.95 (*29*). Myocardial glucose consumption during hyperinsulinemic euglycemia is 47–74 μmole 100 $g^{-1}$ $min^{-1}$ (*30,31*). Assuming a heart mass of 300 g (*32*), myocardial glucose consumption of 50 μmole 100 $g^{-1}$ $min^{-1}$ and total-body glucose metabolic rate of 38.9 μmole $kg^{-1}$ $min^{-1}$ during hyperinsulinemic euglycemia in a 70-kg man (*28,29*), the heart accounts for approximately 5% (150/2,722 = 0.055) of total body glucose metabolism.

Ferrannini et al. (*25*) estimated that the rate of transfer of glucose from blood to the insulin-dependent compartment increased 2.4-fold during hyperinsulinemic euglycemic clamp, whereas the rate to the insulin-independent compartment did not change. I analyzed time-activity curves collected for 50 min after intravenous administration of 1-$^{11}$CG to six macaques. Three were receiving no insulin (plasma glucose 3.6–8.4 m*M*) and three were undergoing hyperinsulinemic clamp (plasma glucose 4.5–7.6 m*M*). The half-time of the fast component showed little difference between the two groups (1.81 ± 0.24 versus 1.98 ± 0.17 min) whereas the half-time of the slow component was shortened by a factor of 1.6 with insulin (42.67 ± 2.1 versus 26.67 ± 5.0 min). Averaging the data from Ferrannini et al. (*25*) in humans and my own data in macaques yields a factor of 2.0 for the increase in glucose transfer rate from blood to the insulin-dependent compartment during hyperinsulinemic clamp.

Based on these data, the clearance of 1-$^{11}$CG from blood to extravascular tissue in normal adults undergoing hyperinsulinemic euglycemia can be described by a slow, insulin-dependent component to heart ($0.05A_0$) and muscle ($0.70A_0$) with a rate constant of 2.08 $hr^{-1}$ (twice normal) and a fast, insulin-independent component to other organs comprising $0.25A_0$ with a rate constant of 32.24 $hr^{-1}$ (normal). For hyperinsulinemic hyperglycemia less than 10 m*M*, the components change to $0.95A_0$ for the insulin-dependent component ($0.05A_0$ to heart and $0.90A_0$ to muscle) and $0.05A_0$ to the insulin-independent compartment. For hyperglycemia greater than 10 m*M*, a third component representing clearance from the blood through the kidneys into the bladder would need to be added.

Subjects with insulin-dependent diabetes mellitus have glucose clearance kinetics similar to normal subjects. Subjects with noninsulin-dependent diabetes mellitus show less shift to muscle uptake during hyperinsulinemia than normal subjects (*28*).

*Blood ($\tilde{A}_{blood}$).* Cumulated activity in blood ($\tilde{A}_{blood}$) is the sum of the integrals of time-activity curves for the slow component to heart and muscle ($\tilde{A}_{bloodHM}$) and the fast component to internal organs ($\tilde{A}_{bloodIO}$). These integrals also must take into account radioactive decay and $[^{11}C]$-$CO_2$ lost via the lungs (Table 1). $\tilde{A}_{blood}$ was apportioned as shown in Table 4 of Powers et al. (*23*) except that 0.108 of the total was taken from high flow organs and ascribed to the heart chamber as per Table 4 of Cloutier and Watson (*33*). This gives the following fractional distribution: lungs 0.196, spleen 0.032, heart chamber 0.108, high flow organs [internal organs apportioned by relative mass (*33*) including heart

wall but excluding spleen and lung] 0.501, and low flow organs (bone, skin, fascia and skeletal muscle) 0.163. This 0.163 fraction was subdivided to muscle 80% (0.130) and bone 20% (0.033) based on the relative masses for ICRP Reference Man (*34*). Of the 20% assigned to bone one-half was assigned to cortical bone and one-half to trabecular bone.

*Heart and Muscle ($\tilde{A}_{HM}$).* Cumlated activity to heart and muscle can be calculated from the fraction of glucose that goes to heart and muscle minus that that remains in blood (Table 1).

*Internal Organs ($\tilde{A}_{IO}$).* Cumulated activity to insulin independent internal organs can be calculated from the fraction of glucose that goes to insulin independent organs minus that which remains in blood (Table 1).

*Apportionment of $\tilde{A}$ to Individual Organs.* Published estimates of glucose uptake to individual organs are quite inconsistent, especially with respect to the brain. Several leave a substantial portion unaccounted for (*25,35,36*). I have allocated $\tilde{A}_{IO}$ to individual insulin-independent organs on the basis of relative mass (*32*). Values were based on organ masses for males for all organs except uterus and ovaries. These values are slightly greater than would be calculated for females due to the smaller total mass of the male internal organs. Skin, breasts, bone and yellow marrow were assumed to have negligible glucose uptake. For $\tilde{A}_{HM}$, constant allocation of 5% $A_o$ to heart was used based on recently published data using $^{18}$FDG that showed no change in myocardial metabolism during hyperinsulinemic euglycemia (*30,31*). This is somewhat inconsistent with the concept of myocardium as an insulin sensitive tissue, but is consistent with the available human data. The remainder of $\tilde{A}_{HM}$ was allocated to muscle.

Cumulated activities for 24 source organs including both intravascular (blood) and extravascular (tissue) components are shown in Table 2.

**TABLE 2**
Source Organ Cumulated Activity
(MBq-hr per MBq $A_o$)

| | EI/EG | HI/EG | HI/HG |
|---|---|---|---|
| Adrenals | 0.0008 | 0.0005 | 0.0003 |
| Brain | 0.0713 | 0.0420 | 0.0293 |
| Gall bladder (wall) | 0.0005 | 0.0003 | 0.0002 |
| Lower large intestine (wall) | 0.0082 | 0.0049 | 0.0034 |
| Small intestine (wall) | 0.0271 | 0.0160 | 0.0113 |
| Stomach (wall) | 0.0078 | 0.0046 | 0.0033 |
| Upper large intestine (wall) | 0.0109 | 0.0064 | 0.0045 |
| Heart contents | 0.0134 | 0.0200 | 0.0245 |
| Heart wall | 0.0111 | 0.0161 | 0.0172 |
| Kidneys | 0.0148 | 0.0088 | 0.0062 |
| Liver | 0.0942 | 0.0558 | 0.0392 |
| Lungs | 0.0668 | 0.0525 | 0.0482 |
| Muscle | 0.0594 | 0.1866 | 0.2383 |
| Ovaries | 0.0004 | 0.0002 | 0.0002 |
| Pancreas | 0.0047 | 0.0028 | 0.0019 |
| Red marrow | 0.0583 | 0.0345 | 0.0243 |
| Cortical bone (surface) | 0.0020 | 0.0030 | 0.0037 |
| Trabecular bone (surface) | 0.0020 | 0.0030 | 0.0037 |
| Spleen | 0.0113 | 0.0087 | 0.0078 |
| Testes | 0.0019 | 0.0011 | 0.0008 |
| Thymus | 0.0010 | 0.0006 | 0.0004 |
| Thyroid | 0.0010 | 0.0006 | 0.0004 |
| Urinary bladder (wall) | 0.0023 | 0.0014 | 0.0010 |
| Uterus | 0.0034 | 0.0020 | 0.0014 |

EI/EG = euinsulinemic euglycemia; HI/EG = hyperinsulinemic euglycemia; HI/HG = hyperinsulinemic hyperglycemia.

## Specific Absorbed Fraction for Blood

Calculations to determine absorbed fraction for positrons for blood irradiating blood ($\phi_{np(blood)}$) were performed according to the method of Cloutier and Watson (*33*). Due to its size, the heart was considered to have $\phi_{np(blood)} = 1$ for its blood contents. The value of $\nu$, the apparent beta particle absorption coefficient, was calculated as 20.12 $cm^{-1}$ in water (*37*). A weighted mean value of $\phi_{np(blood)} = 0.7512$ was determined. The specific absorbed fraction $\Phi_{np(blood)} = 1.35 \times 10^{-4}$ $g^{-1}$ was calculated by dividing by the mass of blood = 5,000 × 1.06 = 5300 g (*27,38*).

## Calculation of Mean Absorbed Dose ($\bar{D}$)

*Target Organ: Blood.* $\bar{D}$ from positrons for blood irradiating itself was calculated for each of the three different conditions from $\tilde{A}_{blood}$, $\Delta_{np}$ and $\Phi_{np\ (blood)}$. $\bar{D}$ from annihilation radiation for blood irradiating blood was calculated from $\tilde{A}_{blood}$, $\Delta_p$ and $\Phi_p$. Values for $\Delta_{np}$ and $\Delta_p$ were obtained from Weber et al. (*20*). $\Phi_p$ was taken as the value for total body to total body $\Phi_p$ for 500 keV photons = $4.97 \times 10^{-6}$ $g^{-1}$ (*39*). Total extravascular cumulated activity for 21 organs and organ-specific S-factors for each organ to total body were used to calculate $\bar{D}$ to blood from other organs. S-factors for contents of gallbladder, upper large intestine, lower large intestine and urinary bladder contents were used for these source organs even though the activity was assumed to reside in the organ walls.

*Target Organ: Other Organs.* $\bar{D}$ for 24 target organs, total body and effective dose for a 70-kg adult were calculated using $\tilde{A}$ in 24 source organs (Table 2) with the computer program MIRDOSE 3 (*40*). S-factors for contents of stomach, gallbladder, upper large intestine, lower large intestine and urinary bladder contents were used for these source organs even though the activity was assumed to reside in the organ walls. Since S-factors for organs irradiating themselves assume $\phi_{np} = 1$, the dose from positron energy absorbed into the blood ($\bar{D}_{\beta+blood}$) was subtracted from the $\bar{D}$ to that organ:

$$\bar{D}_{\beta+(blood)} = \tilde{A}_{blood} \times \Delta_{np} \times \Phi_{np(blood)}.$$

$\tilde{A}_{blood}$ is the cumulated activity in blood assigned to that organ. $\bar{D}_{\beta+(blood)}$ for heart wall and heart chamber were added together and subtracted from the heart wall. This reduced $\bar{D}$ to internal organs from 13% (liver) to 0% (avascular organs—breasts and skin). For muscle, the reduction ranged from 27% to 31%.

*Target Organ: Lens.* As a structure with negligible vasculature and metabolism, $\bar{D}$ to lens was considered to derive entirely from other organs. $\bar{D}$ to lens from organs other than brain was estimated as equal to that received by the brain from other organs. $\bar{D}$ to lens from the brain was calculated using the specific absorbed fraction for adults of $2.45 \times 10^{-5}$ $g^{-1}$ given by Eckerman et al. (*41*) for the eye as the target organ and 500 keV photons arising from brain as the source.

## RESULTS

$\bar{D}$ for 24 organs, total body, lens and blood are shown in Table 3 for euinsulinemic euglycemia, hyperinsulinemic euglycemia and hyperinsulinemic hyperglycemia. Hyperinsulinemia increases $\bar{D}$ to the muscle, heart and blood with a decrease to other internal organs. This effect is more pronounced during hyperinsulinemic hyperglycemia. Heart wall, lungs and spleen are the organs receiving the highest dose, primarily due to the large fractional blood volume assigned to these organs. The increase in $\bar{D}$ to the heart wall during hyperinsulinemia is primarily caused by the increase in $\tilde{A}_{blood}$ in the heart chamber as a consequence of the overall increase in $\tilde{A}_{blood}$. As opposed to lungs and liver, this increase is not accompanied by a decrease in $\tilde{A}$ to the organ tissue. Hyperinsulinemia produces a reduction in effective dose due to the decrease in $\tilde{A}$ in organs with specified weighting factors greater than 0.05.

**TABLE 3**
Radiation Absorbed Dose Estimates for [1-$^{11}$C]-Glucose in Adults (mGy/MBq $A_0$)

| | EI/EG | HI/EG | HI/HG |
|---|---|---|---|
| Adrenals | 0.0146 | 0.0098 | 0.0067 |
| Brain | 0.0160 | 0.0092 | 0.0062 |
| Breasts | 0.0011 | 0.0011 | 0.0011 |
| Gall bladder | 0.0047 | 0.0034 | 0.0028 |
| Lower large intestine | 0.0084 | 0.0055 | 0.0042 |
| Small intestine | 0.0094 | 0.0059 | 0.0044 |
| Stomach | 0.0059 | 0.0044 | 0.0033 |
| Upper large intestine | 0.0083 | 0.0053 | 0.0040 |
| Heart wall | 0.0148 | 0.0207* | 0.0226* |
| Kidneys | 0.0150 | 0.0094 | 0.0069 |
| Liver | 0.0164 | 0.0097 | 0.0068 |
| Lungs | 0.0174† | 0.0136 | 0.0123 |
| Muscle | 0.0011 | 0.0020 | 0.0023 |
| Ovaries | 0.0128 | 0.0072 | 0.0071 |
| Pancreas | 0.0155 | 0.0100 | 0.0074 |
| Red marrow | 0.0072 | 0.0046 | 0.0034 |
| Bone surface | 0.0048 | 0.0034 | 0.0028 |
| Skin | 0.0006 | 0.0007 | 0.0007 |
| Spleen | 0.0182* | 0.0142† | 0.0128† |
| Testes | 0.0125 | 0.0076 | 0.0059 |
| Thymus | 0.0132 | 0.0089 | 0.0068 |
| Thyroid | 0.0126 | 0.0081 | 0.0058 |
| Urinary bladder | 0.0024 | 0.0020 | 0.0018 |
| Uterus | 0.0125 | 0.0080 | 0.0060 |
| Total body | 0.0028 | 0.0027 | 0.0027 |
| Lens | 0.0010 | 0.0009 | 0.0007 |
| Blood | 0.0061 | 0.0078 | 0.0089 |
| Effective dose | 0.0104 | 0.0071 | 0.0060 |

*Primary critical organ.
†Secondary critical organ.
EI/EG = euinsulinemic euglycemia; HI/EG = hyperinsulinemic euglycemia; HI/HG = hyperinsulinemic hyperglycemia.

**TABLE 4**
Dosimetry for Selected Organs Following Administration of Glucose and Glucose Analogs Labeled with Positron-Emitting Radionuclides (mGy/MBq $A_0$)

| | $^{18}$FDG* | $^{11}$CDG† | $^{11}$CG‡ |
|---|---|---|---|
| Brain | 0.028 | 0.0051 | 0.016 |
| Heart wall | 0.043‡ | 0.012 | 0.015 |
| Kidney | 0.026 | 0.011 | 0.015 |
| Liver | 0.021 | 0.007 | 0.016 |
| Lungs | 0.009 | 0.005 | 0.017# |
| Red marrow | 0.011 | 0.003 | 0.007 |
| Spleen | 0.020 | 0.009 | 0.018‖ |
| Testes | 0.013 | 0.013# | 0.012 |
| Urinary bladder | 0.091‖ | 0.035‖ | 0.002 |
| Effective dose | 0.018§ | | 0.010 |

*Dosimetry for $^{18}$FDG using S values for American and European adult reference man (*35*).
†Dosimetry for $^{11}$CDG (*4*).
‡Dosimetry for 1-$^{11}$CG during euglycemic euglycemia from Table 3.
§The effective dose was calculated from individual organ doses for Japanese adults using weighting factors as specified in ICRP 60 (*43*). A 2-hr voiding time was used for the urinary bladder. The mean value for upper and lower large intestine was used for colon. The value for testes was used for gonads. The value for stomach was used for esophagus. The value for other tissue was used for skin.
‖Primary critical organ.
#Secondary critical organ.

## DISCUSSION

Comparing mean absorbed dose estimates for $^{18}$FDG (*35*) and $^{11}$CDG (*42*) to 1-$^{11}$CG during euinsulinemic euglycemia, the main difference is the dose to the bladder wall (Table 4). Glucose is not excreted in the urine at plasma concentrations below 10 m*M* because of complete tubular reabsorption (*21*). $^{18}$FDG and $^{11}$CDG are incompletely absorbed by the tubule after glomerular filtration and substantial quantities are excreted into the bladder urine (*4,42*). Other individual organ doses for $^{11}$CG are higher than those previously reported for $^{11}$CDG and relatively higher than would be expected as compared to $^{18}$FDG given the greater than five-fold longer half-life of $^{18}$F (even taking into account that the S-factors for organ self-irradiation are approximately one and one-half larger for $^{11}$C due to a higher value for $\Delta_{np}$) (*20,38*). This is partly due to the urinary excretion of $^{18}$FDG and $^{11}$CDG, but is also due to differences in assignment of cumulated activity. For the calculations of organ dose after administration of both $^{18}$FDG and $^{11}$CDG, substantial portions of the cumulated activity were not assigned to individual organs but as remainder were assigned to total body: 74.4% for $^{18}$FDG and 62.8% for $^{11}$CDG (*4,40*). In contrast, in this study none of the cumulated activity as remainder to total body but apportioned all the activity to individual organs. Thus, individual organ doses for 1-$^{11}$CG were higher than expected in comparison with both $^{18}$FDG and $^{11}$CDG.

Hyperinsulinemia causes marked changes in the absorbed dose to individual organs from intravenous administration of 1-$^{11}$CG. The hyperinsulinemic insulin clamp technique has been used for studies of myocardial glucose metabolism with PET and $^{18}$FDG (*30,31*). The effect of hyperinsulinemia on the biodistribution of $^{18}$FDG and consequent changes in radiation absorbed dose deserve further consideration.

## CONCLUSION

Use of 1-$^{11}$CG to measure CMRGlc with PET offers advantages over the use of $^{18}$FDG and $^{11}$CDG under conditions where there may be changes in the lumped constant (*18*). Application of 1-$^{11}$CG to PET requires estimation of individual rate constants from dynamically acquired data (*18*). Our initial studies in humans have given excellent precision in estimating regional rate constants with intravenous injections of 333–481 MBq (9–13 mCi), comparable to what we achieve with injections of 370 MBq (10 mCi) of $^{18}$FDG. For more routine imaging procedures, $^{18}$FDG offers the advantage of obtaining a single high-count image of relative CMRGlc with intravenous injections of approximately 185 MBq (5 mCi) (*2–4*). Since the effective dose for $^{18}$FDG is 0.018 mSv/MBq and that for $^{11}$CG is 0.010 mSv/MBq or less, the estimated biological consequences of radiation exposure per study are about the same for both radiopharmaceuticals.

## ACKNOWLEDGMENTS

This work was supported by National Institutes of Health grants NS06833, NS28700 and DK27085.

## REFERENCES

1. Sokoloff L, Reivich M, Kennedy C, et al. The [$^{14}$C]deoxyglucose method for the measurement of local cerebral glucose utilization: theory, procedure and normal values in the conscious and anesthetized albino rat. *J Neurochem* 1977;28:897–916.
2. Huang S-C, Phelps ME, Hoffman EJ, et al. Noninvasive determination of local cerebral metabolic rate of glucose in man. *Am J Physiol* 1980;238:E69–E82.
3. Reivich M, Kuhl D, Wolf A, et al. The [$^{18}$F]Fluorodeoxyglucose method for the measurement of local cerebral glucose utilization in man. *Circ Res* 1979;44:127–137.

4. Reivich M, Alavi A, Wolf A, et al. Use of 2-deoxy-D[1-$^{11}$C]glucose for the determination of local cerebral glucose metabolism in humans: variation within and between subjects. *J Cereb Blood Flow Metab* 1982;2:307–319.
5. Crane PD, Pardridge WM, Braun LD, et al. The interaction of transport and metabolism on brain glucose utilization: a reevaluation of the lumped constant. *J Neurochem* 1981;369:1601–1604.
6. Gjedde A, Diemer NH. Double-tracer study of the fine regional blood-brain glucose transfer in rat by computer-assisted autoradiography. *J Cereb Blood Flow Metab* 1985;5:282–289.
7. Gjedde A. Does deoxyglucose uptake in the brain reflect energy metabolism? *Biochem Pharm* 1987;36:1853–1861.
8. Greenberg JH, Hamar J, Welsh FA, et al. Effect of ischemia and reperfusion on λ of the lumped constant of the [$^{14}$C]deoxyglucose technique. *J Cereb Blood Flow Metab* 1992;12:70–77.
9. Suda S, Shinohara M, Miyaoka M, et al. The lumped constant of the deoxyglucose method in hypoglycemia: effects of moderate hypoglycemia in local cerebral glucose utilization in the rat. *J Cereb Blood Flow Metab* 1990;10:499–509.
10. Dienel GA, Cruz NF, Kentaro M, et al. Direct measurements of the λ of the lumped constant of the deoxyglucose method in the rat brain: determination of λ and lumped constant from tissue glucose concentration or equilibrium brain/plasma distribution for methylglucose. *J Cereb Blood Flow Metab* 1991;11:25–34.
11. Blomqvist G, Gjedde A, Gutniak M, et al. Facilitated transport of glucose from blood to brain in man and the effect of moderate hypoglycemia in cerebral glucose utilization. *Eur J Nucl Med* 1991;18:834–837.
12. Gutniak M, Blomqvist G, Widén L, et al. D-[U-$^{11}$C] glucose uptake and metabolism in the brain of insulin-dependent diabetic subjects. *Am J Physiol* 1990;258:E805–E812.
13. Lifton JF, Welch MJ. Preparation of glucose labeled with 20-min half-lived carbon-11. *Radiation Res* 1971;45:35–40.
14. Mintun MA, Raichle ME, Welch MJ, Kilbourn MR. Brain glucose metabolism measured with PET and U-$^{11}$C-glucose. *J Cereb Blood Flow Metab* 1985;5:S623–S624.
15. Sacks W. Cerebral metabolism of doubly labeled glucose in humans in vivo. *J Appl Physiol* 1965;20:117–130.
16. Blomqvist G, Stone-Elander S, Halldin C, et al. Positron emission tomographic measurements of cerebral glucose utilization using [1-$^{11}$C]D-glucose. *J Cereb Blood Flow Metab* 1990;10:467–483.
17. O'Sullivan F, Muzi M, Spence A, Graham MM. An improved analysis technique for dual tracer PET studies with particular application to lumped constant imaging [Abstract]. *J Nucl Med* 1992;33:944.
18. Powers WJ, Dagogo-Jack S, Markham J, et al. Cerebral transport and metabolism of 1-$^{11}$C-D-glucose during stepped hypoglycemia. *Ann Neurol* 1995;38:599–609.
19. Loevinger R, Budinger TF, Watson EE. *MIRD primer for absorbed dose calculations,* rev. ed. New York, NY: Society of Nuclear Medicine; 1991.
20. Weber DA, Eckerman KF, Dillman LT, Ryman JC. *MIRD:radionuclide data and decay schemes.* New York, NY: Society of Nuclear Medicine; 1989.
21. Pitts RF. *Kidney and body fluids, an introductory text,* 2nd Ed. Chicago, IL:Year Book Medical Publishers Inc.;1968,73–75.
22. Segal S, Berman M, Blair A. The metabolism of variously $^{14}$C-labeled glucose in man and an estimation of the extent of glucose metabolism by the hexose monophosphate pathway. *J Clin Invest* 1961;40:1263–1279.
23. Powers WJ, Stabin M, Howse D, et al. Radiation absorbed dose estimates for oxygen-15 radiopharmaceuticals ($H_2{}^{15}O$,$C^{15}O$,$O^{15}O$) in newborn infants. *J Nucl Med* 1988;29:1961–1970.
24. Comroe JH. *Physiology of respiration.* Chicago, IL: Year Book Medical Publishers; 1965:17–27.
25. Ferrannini E, Smith JD, Cobelli C, et al. Effect of insulin on the distribution and disposition of glucose in man. *J Clin Invest* 1985;76:357–364.
26. Ikkos D, Luft R. On the intravenous glucose tolerance test. *Acta Endocrin* 1957;25: 312–334.
27. Andreoli TE. Disorders of fluid volume, electrolyte and acid-base balance. In: JB Wyngaarden and LH Smith, Jr., eds. *Textbook of medicine,* 18th ed. Philadelphia, PA: WB Saunders Co.;1988;529–558.
28. deFronzo RA. The triumvirate: β-cell, muscle, liver. A collusion responsible for NIDDM. *Diabetes* 1988;37:667–687.
29. Baron AD, Brechtel G, Wallace P, Edelman SV. Rates and tissue sites of non-insulin and insulin-mediated glucose uptake in humans. *Am J Physiol* 1988;255:E769–E774.
30. Knuuti MJ, Nuutila P, Ruotsalainen U, et al. Euglycemic hyperinsulinemic clamp and oral glucose load in stimulating myocardial glucose utilization during positron emission tomography. *J Nucl Med* 1992;33:1255–1262.
31. Hicks RJ, vom Dahl J, Lee KS, et al. Insulin-glucose clamp for standardization of metabolic conditions during F-18 fluoro-deoxyglucose PET imaging [Abstract]. *J Am Coll Cardiol* 1991;17:381A.
32. Christy M. Mathematical phantoms representing children of various age for use in estimates of internal dose. *Oak Ridge National Laboratory report. ORNL/TM-8381/V6.* Springfield, VA: National Technical Information Service U.S. Department of Commerce;1980.
33. Cloutier RJ, Watson EE. Radiation dose from radionuclides in the blood. In: Cloutier RJ, Edwards CL, Snyder WS, Anderson EB, eds. *Medical radionuclides: radiation dose and effects.* Oak Ridge, TN: AEC Symposium Series 20, Conf-691212;1970: 325–346.
34. Snyder WS, Cook MJ, Nasset ES, et al. *Report of the task group on reference man* (ICRP No. 23). New York: Pergamon Press;1974.
35. Mejia AA, Nakamura T, Masatoshi I, et al. Estimation of absorbed doses in humans due to intravenous administration of fluorine-18-fluorodeoxyglucose in PET studies. *J Nucl Med* 1991;32:699–706.
36. Holliday MA. Metabolic rate and organ size during growth from infancy to maturity and during late gestation and early infancy. *Pediatrics* 1971;47:169–179.
37. Loevinger R, Japha EM, Brownell GL. Discrete radioisotope sources. In: Hine GJ, Brownell GL, eds. *Radiation dosimetry.* New York: Academic Press;1956:693–799.
38. Herscovitch P, Raichle ME. What is the correct value for the brain-blood partition coefficient for water? *J Cereb Blood Flow Metab* 1985;5:65–69.
39. Cristy M, Eckerman K. *Specific absorbed fractions of energy at various ages from internal photons sources.* ORNL/TM-8381 V1–V7 Oak Ridge National Laboratory, Oak Ridge, TN;1987.
40. Stabin M. *MIRDOSE 3* Radiation Internal Dose Information Center, Oak Ridge Institute for Science and Education, Oak Ridge, TN, 1994.
41. Eckerman KF, Christy M, Warner GG. Dosimetric evaluation of brain scanning agents. In: Watson EE, Schlafke-Stelson AT, Coffey JL, Cloutier RJ, eds. Third International Radiopharmaceutical Dosimetry Symposium HHS Publication FDA 81–8166, Rockville, MD: FDA;1981:527–540.
42. Jones SC, Alavi A, Christman D, et al. The radiation dosimetry of 2-[F-18]Fluoro-2-deoxy-D-glucose in man. *J Nucl Med* 1982;23:613–617.
43. Huda W, McLellan J, McLellan Y. How will the new definition of 'effective dose' modify estimates of dose in diagnostic radiology? *J Radiology Prot* 1991;11:241–247.